Clinical Cancer Research

Dual Suppressive Effect of miR-34a on the FOXM1/eEF2-Kinase Axis Regulates Triple-Negative Breast Cancer Growth and Invasion

Recep Bayraktar[1], Cristina Ivan[1], Emine Bayraktar[1], Pinar Kanlikilicer[1], Nashwa N. Kabil[1], Nermin Kahraman[1], Hamada A. Mokhlis[1,2], Didem Karakas[1,3], Cristian Rodriguez-Aguayo[1], Ahmet Arslan[4], Jianting Sheng[5], Stephen Wong[5], Gabriel Lopez-Berestein[1,6], George A. Calin[1,6], and Bulent Ozpolat[1,6]

Abstract

Purpose: Recent studies indicated that dysregulation of noncoding RNAs (ncRNA) such as miRNAs is involved in pathogenesis of various human cancers. However, the molecular mechanisms underlying miR-34a are not fully understood in triple-negative breast cancer (TNBC).

Experimental Design: We performed *in vitro* functional assays on TNBC cell lines to investigate the role of miR-34a in FOXM1/eEF2K signaling axis. TNBC tumor xenograft models were used for *in vivo* therapeutic delivery of miR-34a.

Results: In this study, we investigated the role of p53-driven ncRNA miR-34a and found that miR-34a is associated with significantly longer patient survival in TNBC and inversely correlated with levels of proto-oncogenic *eEF2K*, which was associated with significantly shorter overall patient survival. We showed that miR-34a directly binds to the 3′-untranslated region of *eEF2K* and *FOXM1* mRNAs and suppresses their expression, leading to inhibition of TNBC cell proliferation, motility, and invasion. Notably, restoring miR-34a expression recapitulated the effects of inhibition of *eEF2K* and *FOXM1*, the transcription factor for *eEF2K* and the direct target of p53, in TNBC cell lines, whereas overexpression of *eEF2K* and *FOXM1* rescued the effects and signaling pathways mediated by miR-34a. Moreover, *in vivo* therapeutic delivery of miR-34a nanoparticles by systemic intravenous administration delayed tumor growth of two different orthotopic TNBC tumor xenograft models by inhibiting eEF2K and FOXM1, intratumoral proliferation and angiogenesis, and inducing apoptosis.

Conclusions: Overall, our findings provide new insights into the tumor suppressor role of miR-34a by dual-targeting of FOXM1/eEF2K signaling axis and suggest that miR-34a–based gene therapy may be a potential therapeutic strategy in TNBC.
Clin Cancer Res; 24(17); 4225–41.

Introduction

Triple-negative breast cancer (TNBC), which constitutes 15% to 20% of all breast cancers, is associated with an aggressive phenotype and poor clinical outcome, with significantly shorter patient survival times than other breast cancer subtypes. TNBC represents a basal subtype of breast cancer and is characterized by the lack of expression of recognized molecular targets, including estrogen receptor, progesterone receptor, and HER2 (1–3). Patients with TNBC have a greater likelihood of developing distant metastasis, drug resistance, and early relapse (within 2 or 3 years after treatment) than patients with other subtypes of breast cancer (4–6). In addition to the aggressive phenotype of TNBC, poor prognosis is also attributed to lack of molecular targets and significant tumor heterogeneity which has hindered the development of targeted therapies.

miRNAs are a class of small noncoding RNAs that bind to the 3′-untranslated region (3′-UTR) of target genes (i.e., mRNA) and negatively regulate expression of protein-encoding genes (7). Recent studies indicated that dysregulation of miRNAs is involved in the pathogenesis of diseases such as cancer by controlling multiple cell signaling pathways, including apoptosis, angiogenesis, cell-cycle arrest, senescence, migration, metastasis, and tumorigenesis (8–14). In mammals, the miR-34 family includes three miRNAs that are encoded by two different genes. miR-34a is encoded by its own transcript, whereas miR-34b and miR-34c share a common transcript and are dysregulated in some cancers (15, 16). The miR-34 family is a direct target of the p53 network

[1]Department of Experimental Therapeutics, The University of Texas- MD Anderson Cancer Center, Houston, Texas. [2]Department of Pharmacology and Toxicology, Faculty of Pharmacy, The University of Al-Azhar, Cairo, Egypt. [3]Department of Clinical Biochemistry, Faculty of Medicine, Istinye University, Istanbul, Turkey. [4]Department of Medical Genetics, Faculty of Medicine, Namik Kemal University, Tekirdag, Turkey. [5]Department of Systems Medicine & Bioengineering, Methodist, Houston, Institute for Academic Medicine Research Institute Houston Methodist Weill Cornell Medical College, Houston, Texas. [6]Center for RNA Interference and Non-Coding RNAs, The University of Texas MD Anderson Cancer Center, Houston, Texas.

Note: Supplementary data for this article are available at Clinical Cancer Research Online (http://clincancerres.aacrjournals.org/).

Corresponding Author: Bulent Ozpolat, The University of Texas MD Anderson Cancer Center, 1515 Holcombe Boulevard, Houston, TX 77030. Phone: 713-563-0166; Fax: 713-792-0362; E-mail: Bozpolat@mdanderson.org

doi: 10.1158/1078-0432.CCR-17-1959

Translational Relevance

miR-34a has been shown to target and inhibit several oncogenic genes/proteins. However, the molecular mechanisms underlying its tumor suppressor effects are not fully understood. Our findings are the first to report a dual negative regulatory effect of miR-34a on FOXM1/eEF2K oncogenic signaling axis in TNBC through a direct binding and targeting of eEF2K and FOXM1. *In vivo* nanoliposomal delivery of miR-34a inhibits tumor growth in orthotopic TNBC models. Restoration of miR-34a and targeting the FOXM1/eEF2K axis may be a potential therapeutic approach against TNBC.

(15, 16) and has been shown to target (inhibit) genes, including Wnt, Notch1, CDK4-6, SIRT1, and Bcl-2 in estrogen receptor–positive breast cancer cells (17–20). Although a miR-34–based therapeutics were the first-in-class miRNA therapy to reach clinical trials in melanoma (21), its expression, clinical significance, and molecular mechanisms in TNBC remains to be elucidated.

Eukaryotic Elongation factor 2 kinase (eEF2-kinase, EF2K, eEF2K), an atypical member of alpha kinase family, plays a role in control of peptide elongation phase of protein synthesis (22). eEF2K is highly overexpressed in TNBC patient tumors and cell lines and promotes cell proliferation, motility/invasion, and tumorigenesis (23). Moreover, its direct genetic inhibition in orthotopic TNBC tumor models significantly suppresses tumor growth and enhances the efficacy of chemotherapy (23, 24), suggesting that eEF2K could be a potential molecular therapeutic target in TNBC.

In this study, we found that the expression of miR-34a expression was reduced in TNBC cells and associated with the significantly longer overall patient survival, indicating a tumor suppressor function in patients with TNBC. miR-34a was inversely correlated with *eEF2K* expression, which was also associated with shorter patient survival. Restoration of miR-34a *in vitro* and *in vivo* tumor models of TNBC cells suppressed cell proliferation, invasion, and tumorigenesis through targeting FOXM1/eEF2 signaling axis. Overall, *in vivo* therapeutic delivery of miR-34a could be a potential therapeutic strategy to control TNBC.

Materials and Methods

Cell lines and cell culture conditions

The human mammary epithelial cell lines HMEC and MCF-10A; TNBC cell lines MDA-MB-231, MDA-MB-436, MDA-MB-468, BT-483, SUM-149, and HCC1937; and HEK293 cells were purchased from ATCC. MDA-MB-231, MDA-MB-436, MDA-MB-468, BT-483, and HEK293 cells were cultured in DMEM/F12 medium supplemented with 10% FBS and a 100-U/mL penicillin–streptomycin solution (Sigma). SUM-149 cells were cultured in DMEM/F12 medium supplemented with 5% FBS, 1 μg/mL hydrocortisone (Sigma), 5 μg/mL insulin (Sigma), and 100-U/mL penicillin–streptomycin solution. HCC1937 cells were cultured in RPMI1640 medium supplemented with 10% FBS and 100-U/mL penicillin–streptomycin solution. MCF-10A and HMEC cells were maintained in a nutrient mixture consisting of DMEM/F12 medium supplemented with 5% horse serum, epidermal growth factor, hydrocortisone, insulin, and cholera toxin. All cultured cells were incubated at 37°C in a water-saturated 95% air–5% CO_2 atmosphere.

Expression of miR-34a in breast cancer patient samples and Kaplan–Meier survival analyses

We utilized the Cancer Genome Atlas (TCGA) database to determine the expression profile of miR-34a in patients with breast cancer using the Agilent Technologies miRNA profiling system. The assay uses 100 ng of nonfractionated total RNA, which is directly labeled by ligation of a Cy3-labeled pCp molecule to the 3′ end of the RNA. The labeled cytosine interacts with the guanidine at the 5′ end of the probe, which adds stability to the hybridization complex. In addition, the probes are designed to provide both sequence and size discrimination, generally resulting in highly specific detection of closely related mature miRNAs. The labeling and probe design strategies allow for a precise and accurate measurement that spans a linear dynamic range of greater than four orders of magnitude from at least 0.2 amol to 2 fmol of miRNA and a detection limit of less than 0.1 amol (25). For the miRNA-Seq data, we derived the "reads per million miRNA mapped" values for the mature form miR-34a from the file "illuminahiseq_mirnaseq-miR_isoform_expression" from the Broad Institute (Cambridge, MA; http://gdac.broadinstitute.org/). We identified 61 TCGA patients for whom clinical and miRNA data were available. A Cox regression analysis revealed that, when miR-34a levels were stratified by the median level, lower levels of miR-34a were associated with poor OS for patients with TNBC (HR 0.19; 95% confidence interval, 0.04–0.89; P[log-rank test] = 0.014). Kaplan–Meier plots were generated for the median cutoff.

The reverse-phase protein array (RPPA) levels of eEF2K for TCGA patients with breast cancer were retrieved from the TCPA portal (http://tcpaportal.org/tcpa/). For Basal-like/TNBC cases, a Cox regression analysis revealed significant associations between overall survival and eEF2K as a continuous variable. The analysis yielded an HR of 4.47 [95% CI, 1. 07–18.56; Wald test P-value = 0.01). We then used the log-rank test to find the point (cut-off) with the most significant (lowest P value) split in high versus low RPPA level groups. The Kaplan–Meier plots were generated for this cutoff (0.75). The numbers of patients at risk in low and high eEF2K groups at different time points are presented at the bottom of the graph.

Cell viability and colony formation assays

Proliferation of MDA-MB-231 and MDA MB-436 cells was analyzed by the 3-(4,5-dimethylthiazol-2-yl)-5-(3-carboxymethoxyphenyl)-2-(4-sulfophenyl)-2H-tetrazolium (MTS) assay as described previously (26). Cells were seeded at a density of 1 to 2×10^3 cells/well in 96-well plates and incubated overnight, then treated with either miRNA mimic or scrambled negative control miRNA (Ambion). MTS dye (5 mg/mL) was added at 24, 48, and 72 hours and plates were analyzed on a VMax kinetic ELISA microplate reader (Molecular Devices) and read at 490 nm wavelength.

Clonogenic assay was performed by preparing single-cell suspensions of MDA-MB-231 and MDA-MB-436 cells, then seeding 250 cells/well in 24-well tissue culture plates. After incubation for 48 hours, cells were transfected with miR-34a mimic or control mimic (Ambion) and *eEF2K* or *FOXM1* siRNA or control siRNA (Sigma) and cultured for 10-14 days. Colonies were then stained with crystal violet and quantified by using

ImageJ software. Each experiment was performed independently in triplicate.

Transfections with miRNA mimics/inhibitor or siRNAs

MDA-MB-231 and MDA-MB-436 cells were seeded at a density of 1.5×10^5 cells/well in six-well culture plates and transfected with 50 nmol/L miR-34a mimic/inhibitor-antagomiR or scrambled negative control miRNA mimic/inhibitor (50 nmol/L; Ambion) using HiPerFect transfection reagent (Qiagen) in Opti-MEM reduced serum medium (Life Technologies) according to the manufacturer's instructions (mature miR-34a sequence: UGGCAGUGUCUUAGCUGGUUGU). Other cells were transfected with 50 nmol/L *eEF2K* siRNA, *FOXM1* siRNA, or control siRNA according to the manufacturer's recommended protocol (Sigma). After 6 hours of incubation, medium was replaced with DMEM supplemented with 10% FBS and cells were incubated for up to 72 hours.

Establishment of stably *eEF2K*- and *FOXM1*-overexpressing cells

MDA-MB-231 cells were transfected with lentiviral plasmids containing the specified lentiviral vector for *eEF2K* (NM_013302.3) and *FOXM1* (NM_202002.2) with the CMV promoter (LPP-U0633-Lv105; GeneCopoeia) or the mock vector (LPP-NEG-Lv103; GeneCopoeia) according to the manufacturer's instructions. eEF2K and FOXM1 protein expressions were verified by the Western blotting.

miRNA and mRNA reverse transcription and qPCR analyses

Total RNA was extracted using the miRNeasy Mini Kit (Qiagen) according to the manufacturer's recommended protocol and reverse-transcribed to complementary DNA (cDNA) using the qScript microRNA cDNA Synthesis Kit (Quanta BioSciences). miR-34a expression was measured by qRT-PCR using the PerfeCTa microRNA Assay Kit (Quanta BioSciences) and normalized to U6 small nuclear RNA (Quanta BioSciences) as an endogenous control. For *eEF2K* gene expression, reverse-transcription was performed with a RevertAid First-Strand cDNA Synthesis Kit (Thermo Scientific). *eEF2K* gene expression was measured with the iQ SYBR Green Supermix qPCR Kit (Bio-Rad). The sequences of the sense and antisense *eEF2K* primers were 5′-GGAGAGAGTCGAAGGTCACG-3′ and 5′- GCAATCAGC CAAGACCATCT-3′, respectively. The sequences of the sense and antisense *FOXM1* primers were 5′-CCTTCTGGACCATTCACCCC-3′ and 5′-TCGGTCGTTTCTGCTGTGAT-3′, respectively. The sequences of the sense and antisense GAPDH primers were 5′-CAAGGTCAT CCATGACAACTTTG-3′ and 5′-GTCCACCACCCTGTTGCTGTAG-3′, respectively. cDNA synthesis was verified by detection of the *GAPDH* transcript, which was used as an internal control. Relative differences in expression were determined using the comparative threshold cycle ($2^{-\Delta\Delta CT}$) method.

Protein extraction and Western blotting

MDA-MB-231 and MDA-MB-436 cells were transfected with either miR-34a mimic or control mimic, *eEF2K* siRNA, *FOXM1* siRNA, or control siRNA; cell lysates were collected 72 hours after transfection and subjected to the Western blot analysis according to a method described previously (23, 26, 27). Protein expression levels were detected by using specific antibodies for eEF2K, p-EF2^{Thr56}, SRC, p-SRC^{Tyr416}, FOXM1, c-MYC (all, Cell Signaling Technology), FAK, p-FAK^{Tyr397} (B&D Biosciences), p-AKT^{Ser473}, AKT, cyclin D1 (Santa Cruz Biotechnology), and their corresponding horseradish peroxidase–conjugated secondary antibodies (23, 26, 27). β-Actin (Sigma) was used as a loading control. All experiments were repeated three times independently.

Reverse-phase protein array

MDA-MB-231 and MDA-MB-436 cells treated with either miR-34a mimic or control mimic were subjected to RPPA at the Functional Proteomics RPPA Core Facility of The University of Texas MD Anderson Cancer Center according to the method described previously (26, 28).

Cell motility, migration, and invasion assays

MDA-MB-231 and MDA-MB-436 cells were seeded at a density of 1×10^5 cells/well in six-well culture plates, and after incubation for 24 hours were transfected with miR-34a mimic, *eEF2K* siRNA, a combination of the two, or a combination of control miRNA and control siRNA. The cells were then placed in the upper chambers of gelatin (Sigma)-coated transwell inserts with 8-μmol/L pore size (Corning); the cells were allowed to migrate to the lower chambers to determine their motility and migration capacity. The invasive capacity of these transfected cells was determined by a similar experiment in which the transwell chamber inserts were coated with Matrigel matrix (both from Corning). Cells were seeded at a density of 1×10^5 cells/well in serum-free medium in the top chamber inserts and incubated for 24 hours. The cells were then allowed to invade into the bottom chambers, which contained medium supplemented with 10% FBS. Inserts were then fixed and stained with Hema 3 (Thermo Scientific), and the numbers of invaded or migrated cells were counted in five different fields using a light microscope. All experiments were performed in triplicate.

Luciferase reporter assay for miR-34a-target gene binding and expression

MDA-MB-231, MDA-MB-436, and HEK293 cells were transfected with pEZX-MT06 miRNA reporter vectors containing the binding sites for miR-34a in the 3′-Untranslated regions (3′-UTR) of *FOXM1* and *eEF2K* and the luciferase gene (GeneCopoeia). pEZX-MT06 miRNA reporter vectors containing one point mutation at the miR-34a binding site (*eEF2K*- CACTGCC→TATGACT) and (*FOXM1* AGAGACTGCC> GACAATCAAC) were transfected as a control for target specificity of gene expression. Cells were plated (5×10^4 cells/well) in each well of a 24-well plate 24 hours before transfection. The cells were transfected with the pEZX-MT06 vector (200 ng) together with 50 nmol/L miR-34a mimic or control miRNA. Luciferase activity was measured 48 hours after transfection by the Luc-Pair miR Luciferase Assay (GeneCopoeia). For each sample, firefly luciferase activity was normalized to *Renilla* luciferase activity.

Orthotopic xenograft TNBC mouse models

Female nude athymic mice (4–5 weeks old) were obtained from the Department of Experimental Radiation Oncology, MD Anderson Cancer Center. All studies were conducted according to the experimental protocol approved by the MD Anderson Institutional Animal Care and Use Committee. Each mouse was injected with MDA-MB-231 or MDA-MB-436 cells (2×10^6 in 20% matrigel) into the mammary fat pad. After approximately

2 weeks, when tumor size was 3 to 5 mm, treatment with nanoliposome-encapsulated miRNA was started. miR-34a or control miRNA was incorporated into liposomes composed of 1,2-dimyristoyl-sn-glycero-3-phosphocholine (DMPC) and pegylated distearoyl-phosphatidylethanolamine (DSPE-PEG-2000; Avanti Lipids) at a dose of 0.3 mg/kg equivalent (8 μg/mouse) once a week in a volume of 100 μL (26, 27). Treatments were administered by weekly tail vein injection for 4 weeks (total of four injections). Tumor volumes were measured weekly using an electronic caliper. After completion of the treatment protocol, mice were euthanized and weighed to measure tumor growth. Tumor tissues were collected and subjected to the Western blot analysis, IHC, and terminal deoxynucleotidyl transferase–mediated dUTP nick end labeling (TUNEL) analyses.

Blood samples and clinical biochemistry analyses for *in vivo* toxicity

Female CD-1 IGS mice (4–5 weeks old) were obtained from the Jackson Laboratories (Portland, ME). miR-34a mimic or control miRNA was incorporated into liposomes. Blood samples were collected 24 hours after the treatments and placed into a serum separator tubes for the analysis of toxicity. Serum biochemical parameters for kidney, liver, and blood toxicity were measured for each animal by the Department of Veterinary Medicine and Surgery, MD Anderson Cancer Center. These parameters included blood urea nitrogen (BUN), glucose, aspartate aminotransferase (AST), alanine aminotransferase (ALT), creatinine, total bilirubin, and lactic dehydrogenase (LDH).

IHC

Formalin-fixed, paraffin-embedded tumor samples from the tumors resected from the mice were sectioned (5 μm) and stained with hematoxylin and eosin. Immunostaining for Ki-67 and CD31 was performed to evaluate cell proliferation and angiogenesis, respectively, according to the manufacturer's protocol. The slides were analyzed by microscopy (Nikon Eclipse TE-200-U; Nikon Instruments, Inc.).

TUNEL assay

DNA fragmentation detected in apoptotic cells was measured by TUNEL assay according to the manufacturer's instructions. Tumor tissue sections were incubated with biotin-dUTP and terminal deoxynucleotidyl and counterstained with Hoechst 33342 dye (Thermo Scientific) to detect DNA fragmentation. Positively stained cells were examined by inverted fluorescence microscope and the number of TUNEL-positive cells in five fields per section was quantified.

Statistical analyses

Data were expressed as mean ± SDs. ANOVA was used to compare the control and treatment groups. All values were analyzed using the two-tailed Student *t* test. *P* values <0.05 were considered statistically significant. Analyses were performed using GraphPad Prism (version 6.02) software. Survival analyses were performed in R (version 3.0.1; http://www.r-project.org/). Patients were grouped into percentiles according to mRNA/miRNA expression. The log-rank test was used to determine the association between mRNA/miRNA expression and overall survival, and the Kaplan–Meier method was utilized to generate survival curves.

Results

Reduced miR-34a expression is associated with poor overall patient survival in TNBC

To elucidate the clinical significance of miR-34a expression, we analyzed a TNBC subset of patients from TCGA database. Kaplan–Meier survival curves were plotted according to miR-34a expression levels to assess prognosis. The OS rate was dramatically higher in patients with high miR-34a expression than in patients with low miR-34a expression ($n = 61$; $P = 0.0141$; Fig. 1A).

miR-34a expression is reduced in TNBC cell lines

First, we analyzed the basal expression level of miR-34a in TNBC cells lines by quantitative reverse-transcriptase PCR (qRT-PCR) and compared it to that in normal human mammary epithelial cell line MCF-10A. Our results show that miR-34a basal expression level was significantly lower in TNBC cells lines than in MCF-10A cells (Fig. 1B).

eEF2K expression is inversely correlated with miR-34a expression in TNBC cells and associated with poor survival in patients

To identify potential oncogenic targets of miR-34a, we used various algorithms that predict the possible miR interactions based on bindings sites on 3′-UTR of the target genes, including TargetScan (http://www.targetscan.org/vert_72/), Diana tools (http://diana.imis.athena-innovation.gr/DianaTools/index.php), and microRNA.org (http://www.targetscan.org/vert_72/). Among the potential target mRNAs, *eEF2K* encoding eEF2-kinase was identified by presence of the most common binding site of miR-34a. RT-PCR analysis revealed that basal *eEF2K* expression was higher in TNBC cells lines than in MCF-10A (Fig. 1C), suggesting an inverse relationship between *eEF2K* and miR-34a expression, and the possibility that miR-34a regulates *eEF2K* mRNA expression.

Next, we determined the clinical significance and prognostic value of eEF2K protein expression by analyzing a cohort from the TCGA breast cancer database. OS curves were plotted by using the Kaplan–Meier method according to eEF2K protein expression levels in patients for whom these levels were available (Supplementary Table S1). Overall survival rate was significantly lower in patients whose tumors expressed high levels of eEF2K than in patients whose tumors expressed low levels of eEF2K ($P = 0.0135$; Fig. 1D).

miR-34a directly binds to the 3′-UTR region of eEF2K mRNA to regulate its expression

To examine the direct role of miR-34a on *eEF2K* mRNA regulation, we identified the consensus sequences on the 3′-UTR region of the *eEF2K* gene for binding to miR-34a (Fig. 1E). MDA-MB-231 and MDA-MB-436 TNBC cells were transfected with miR-34a mimic or control mimic oligonucleotides (Supplementary Fig. S1A) and collected at 48 hours for qRT-PCR analysis and at 72 hours for the Western blot analysis. As shown in Fig. 1F, miR-34a negatively regulated *eEF2K* mRNA levels in both cell lines. Western blot analysis revealed that miR-34a significantly decreased expression of the eEF2K protein and of the active form of its immediate downstream target p-EF2^{Thr56} compared with untreated or control mimic–treated MDA-MB-231 and MDA-MB-436 cells (Fig. 1G).

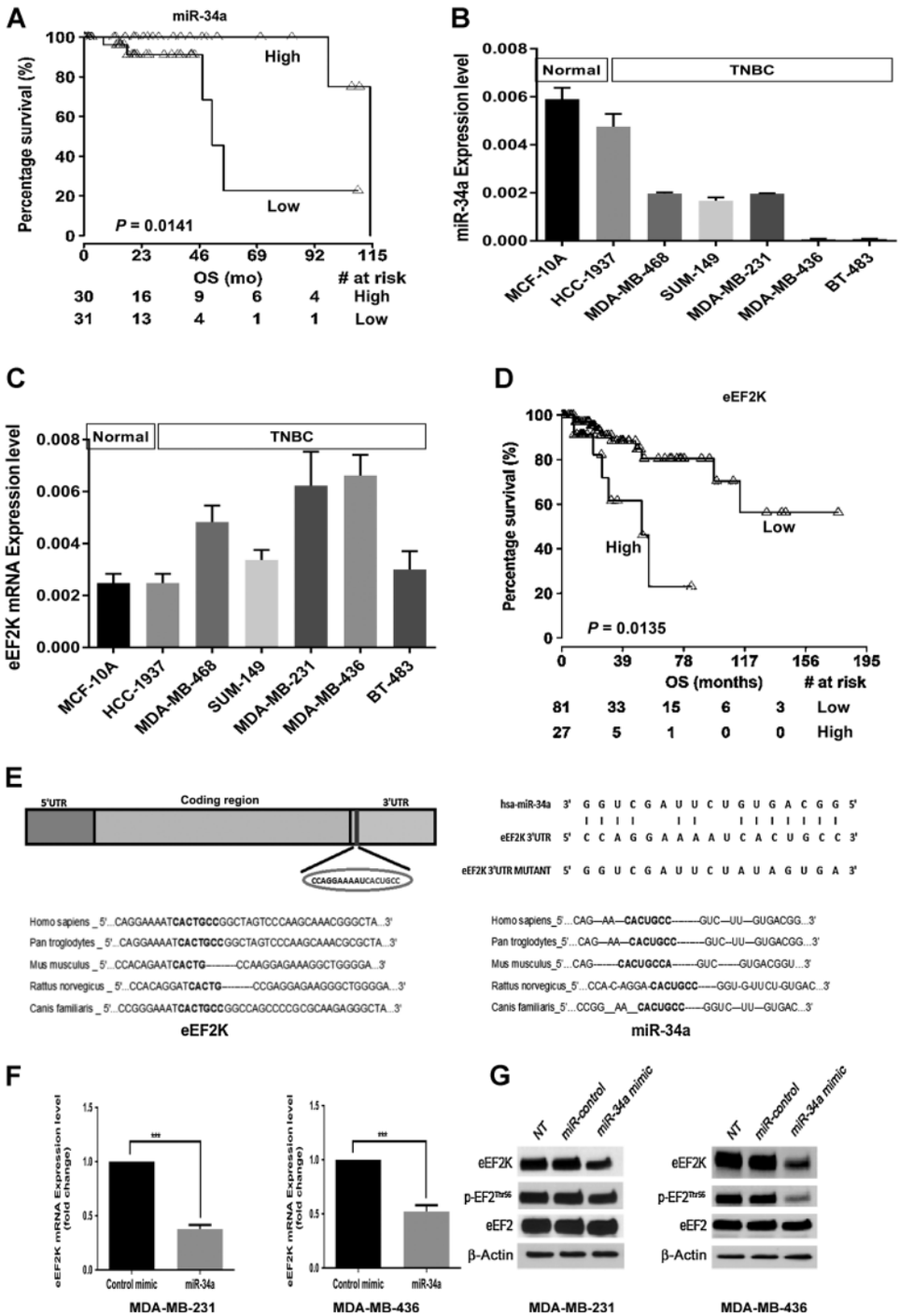

Figure 1.

miR-34a expression is reduced in patients with TNBC and cell lines and reduced miR-34a is correlated with poor overall survival. **A,** Reduced expression of miR-34a is correlated with poor OS in patients with TNBC (TCGA database) as determined by Kaplan–Meier analysis ($P = 0.014$). The numbers of patients at risk in the low and high miR-34a groups at different time points are presented at the bottom of the graph. Mo, months. **B,** Expression levels of miR-34a in TNBC cell lines and normal breast epithelial MCF-10A cells were determined by qRT-PCR. **C,** Expression levels of *eEF2K* mRNA in TNBC cell lines were determined by qRT-PCR. Data were normalized to the expression of *GAPDH* and represent mean + SDs of three independent experiments. **D,** Increased eEF2K protein expression is correlated with poor OS in patients with TNBC/basal-type breast cancer (TCGA database) by Kaplan–Meier survival analysis. **E,** Predicted binding site of miR-34a in the 3′-UTR of human wild-type *eEF2K* and their sequences were determined. Mutations in the seed sequence of the full-length *eEF2K* 3′-UTR is also shown. The predicted miR-34a binding site in eEF2K 3′UTR is highly conserved in mammals. **F** and **G,** Ectopic expression of miR-34a in MDA-MB-231 and MDA-MB-436 cells led to decreased *eEF2K* mRNA expression levels by qRT-PCR (**F**) and decreased eEF2K protein expression levels by the Western blotting (**G**). NT, no treatment.

To further prove that miR-34a–induced suppression of *eEF2K* mRNA expression is mediated through its direct binding to the predicted site in the 3′-UTR of the *eEF2K* gene, we performed a luciferase gene reporter assay. The binding site for miR-34a in the *eEF2K* 3′-UTR was cloned into a pEZX-MT06 miRNA reporter vector which also contains the luciferase gene (pEZX-MT06-3′-UTR). A similar vector (pEZX-MT06-3′-UTR-MT) containing a point mutation in the miR-34a binding site of the *eEF2K* 3′-UTR was used as a negative control. The resulting plasmids were cotransfected into HEK293, MDA-MB-231, and MDA-MB-436 cells along with the miR-34a mimic or the miRNA mimic control. Luciferase activity was significantly decreased in cells transfected with the plasmid containing the binding site for miR-34a ($P < 0.0001$; Fig. 2A), whereas no change in luciferase activity was observed in cells transfected with the plasmid containing mutated binding site and miR-34a. These findings suggest that miR-34a directly recognizes and binds to the *eEF2K* 3′-UTR, specifically in the predicted binding site, to suppress the expression of *eEF2K* mRNA.

miR-34a inhibits proliferation and cell cycle in TNBC cells

To examine the short-term effects of miR-34a on proliferation of TNBC cells, we performed the MTS assay with MDA-MB-231 and MDA-MB-436 cells (72 hours). miR-34a transfection led to greater expression of miR-34a than in the corresponding control miR-transfected cells (Supplementary Fig. S1A) and inhibited proliferation of both cell types (MDA-MB-231, $P = 0.0007$; MDA-MB-436, $P = 0.036$; Fig. 2B). Ectopic overexpression of miR-34a had no significant reduction in cell proliferation and cell viability in normal breast epithelial cells HMEC and MFC10A (72 hours; Supplementary Fig. S1B). We further examined the effects of miR-34a on TNBC cell proliferation and clonogenicity using a colony formation assay. miR-34a expression significantly decreased colony formation in both MDA-MB-231 ($P = 0.0008$) and MDA-MB-436 ($P = 0.0001$) cells compared with untreated or control miR–transfected cells (Fig. 2C).

To investigate the effects of miR-34a on cell-cycle progression, TNBC cells were treated with miR-34a or control mimic and subjected to flow cytometry for cell-cycle analysis. Treatment of MDA-MB-231 and MDA-MB-436 cells with miR-34a significantly increased the percentage of cells in G_1 phase and significantly decreased the percentage of cells in S phase compared with untreated or control miR–transfected cells (Fig. 2D). This suggests that miR-34a plays a role in regulation of cell-cycle progression in TNBC cells.

miR-34a inhibits cell proliferation through downregulation of eEF2K signaling

To show that the effects of miR-34a on cell proliferation and signaling pathways in TNBC cells are mediated by eEF2K, we performed a clonogenic assay. *eEF2K* silencing recapitulated the effects of miR-34a expression and inhibited clonogenic cell growth in MDA-MB-231 ($P = 0.0002$) and MDA-MB-436 ($P = 0.0002$) cells (Fig. 3A). miR-34a expression and EF2K silencing increased p27 and cyclin E and CDK2, regulators of G_1- to S-phase transition, in both cell lines (Fig. 3B). Unbiased RPPA analysis revealed that miR-34a transfection decreased the activity and expression of FOXM1, c-myc, CDK1, p-4E-BP1, Chk1, Myt1, Notch1 and, p-SRC, in MDA-MB-436 cells (Fig. 3C; Supplementary Table S2). To validate our RPPA results, we performed the Western blot analysis in MDA-MB-231 and MDA-MB-436 cells. Our results revealed that treatment of these cells with miR-34a or *eEF2K* siRNA reduced the expression of p-SRC^{Tyr416}, p-FAK^{Tyr397}, p-4E-BP1$^{Tyr37\text{-}T47}$, and c-myc compared with untreated or miR control–transfected control cells (Fig. 3D and E). Knockdown of *eEF2K* with siRNA had similar effects on expression levels of these proteins, suggesting that miR-34a–mediated effects can be attributed to regulation of *eEF2K* in TNBC and that, overall, the effects of miR-34a are mediated through downregulation of *eEF2K*.

miR-34a targets FOXM1/eEF2K axis to mediate its effects in TNBC cells

The oncogenic transcription factor *FOXM1*, a p53-regulated (suppressed) gene, and its target *eEF2K* have been shown to be the major oncogenic drivers in TNBC (8–16). We have shown that *FOXM1* regulates *eEF2K* expression by binding to its promoter region (27), suggesting an existence of *miR-34a/FOXM1/EF2K* signaling axis. Furthermore, miR-34a was previously shown to mediate its tumor suppressor effects by directly binding and inhibiting *FOXM1* in hepatocellular carcinoma (29). Thus, we hypothesized that in addition to its direct regulatory effect on *eEF2K*, miR-34a mediated suppression of *eEF2K* gene expression could also be reinforced through downmodulation of *FOXM1*. In fact, the results of RPPA, the Western blot analysis, and qRT-PCR analysis provided the first evidence that miR-34a expression suppressed FOXM1 expression in both TNBC cells (MDA-MB-231 and MDA-MB-436; Fig. 4A and B) and highly interactive important pathways (Fig. 3C). To determine whether the negative regulatory effect of miR-34a on *FOXM1* expression is mediated through direct binding to the predicted sites in the 3′-UTR of the *FOXM1* (Fig. 4C), cells were cotransfected with the plasmid containing the binding site in the 3′-UTR of *FOXM1* and miR-34a. To further provide proof of the binding of miR-34a to the specific binding motifs, we also introduced point mutations (AGAGACTGCC > GACAATCAAC) into the corresponding miR-34a binding site in the 3′-UTR of *eEF2K* or *FOXM1*. Luciferase activity representing the miR-34–regulated expression of *eEF2K or FOXM1* was significantly decreased in HEK293, MDA-MB-231, and MDA-MB-436 cells, which were transfected with the plasmid containing the binding site for miR-34a (Fig. 4D). No change in luciferase activity was observed in cells transfected with the plasmid containing mutated binding site and miR-34a. Because FOXM1 was previously reported to play a critical role in cell proliferation and cell-cycle progression in TNBC cells (27), silencing *FOXM1* by siRNA mimicked the effects of miR-34a and significantly inhibited clonogenic cell growth (Fig. 4E) with a concomitant decrease in eEF2K expression, and altered expression levels of cell proliferation and cell-cycle mediators, such as CDK2, cyclin E1, and p27 as well as p-(Tyr 397)-FAK (Fig. 5A).

miR-34a inhibits cell migration and invasion of TNBC through eEF2K inhibition

Considering the role of miR-34a in regulation of eEF2K and SRC/FAK, which are known to promote cell motility and invasion, we investigated the role of miR-34a in TNBC cell migratory and invasive capacities. MDA-MB-231 and MDA-MB-436 cells were transfected with miR-34a, *eEF2K* siRNA, and subjected to migration and invasion assays utilizing transwell invasion chambers. Given the incomplete target silencing with the miRNA alone, we questioned whether the combination of siRNA and miRNA that target the same pathway would enhance the efficacy of miR-34a–

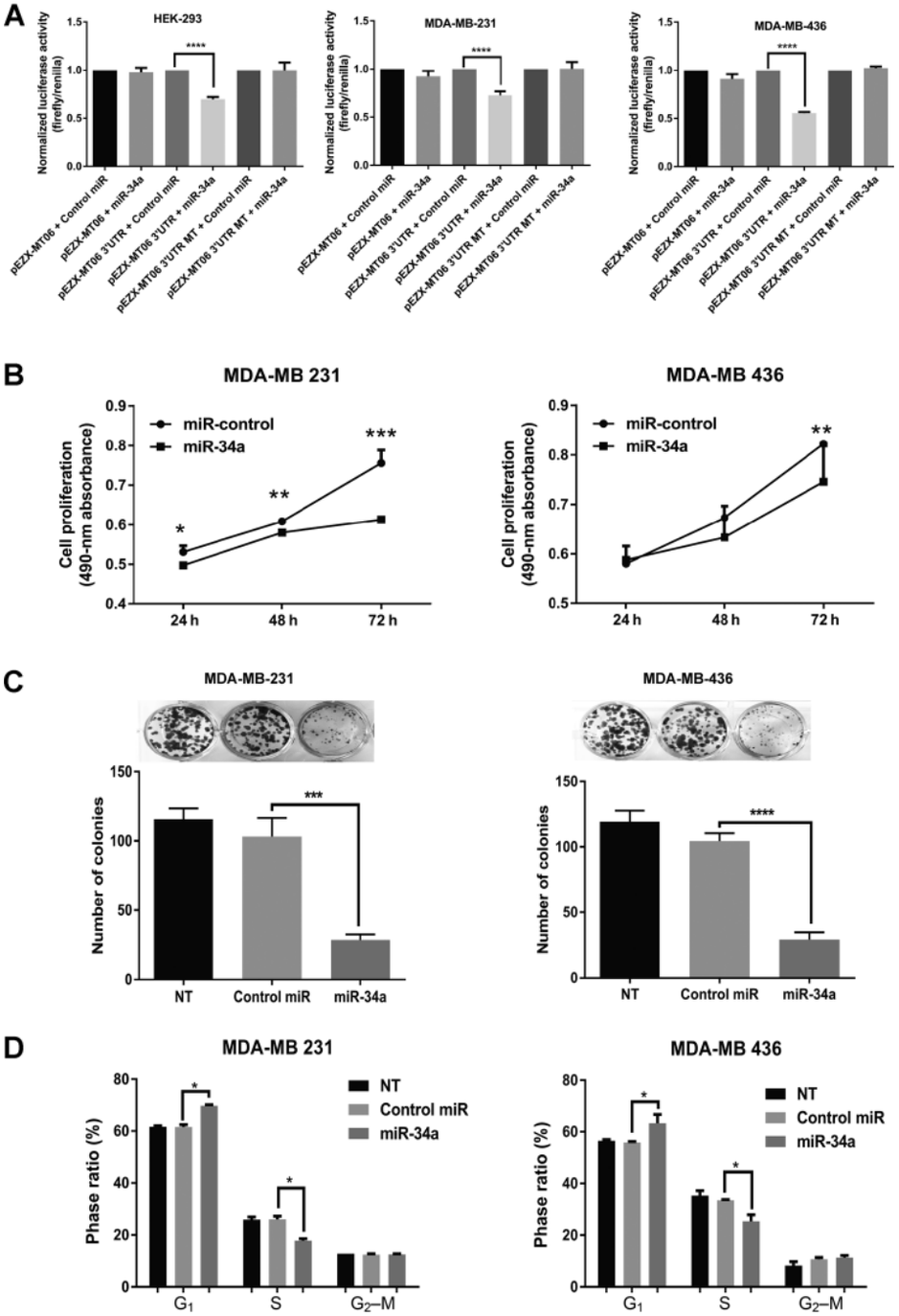

Figure 2.

miR-34a directly binds to 3′-UTR of eEF2K mRNA and suppresses its expression and inhibits cell proliferation and cell cycle in TNBC cells. **A,** Luciferase reporter assay results show that miR-34a directly targets the *eEF2K* 3′-UTR-luciferase reporter (wild-type binding site) in HEK-293, MDA-MB-231, and MDA-MB-436 cells. The firefly luciferase activity of the reporter was normalized to the internal *Renilla* luciferase activity. Data are presented as mean + SDs for three independent experiments. ***, $P < 0.0001$. **B,** The short-term effects of ectopic expression of miR-34a on the proliferation of MDA-MB-231 and MDA-MB-436 cells was examined by the MTS assay, and the mean absorbance at 490 nm was determined at 24, 48, and 72 hours. Data represent mean ± SDs. **C,** Effects of overexpression of miR-34a on the clonogenic ability of MDA-MB-231 and MDA-MB-436 cells were determined by a colony-formation assay. Top panels are representative images from the colony formation assay, and bottom panels represent quantification of the number of colonies formed. The data are mean ± SDs. **D,** Determination of cell-cycle distribution after treatment with miR-34a or control miRNA or no treatment (NT) shows that miR-34a increased the number of TNBC cells in G_1 phase and decreased the percentage of cells in S phase. *, $P < 0.05$; **, $P < 0.01$; ***, $P < 0.001$; ****, $P < 0.0001$.

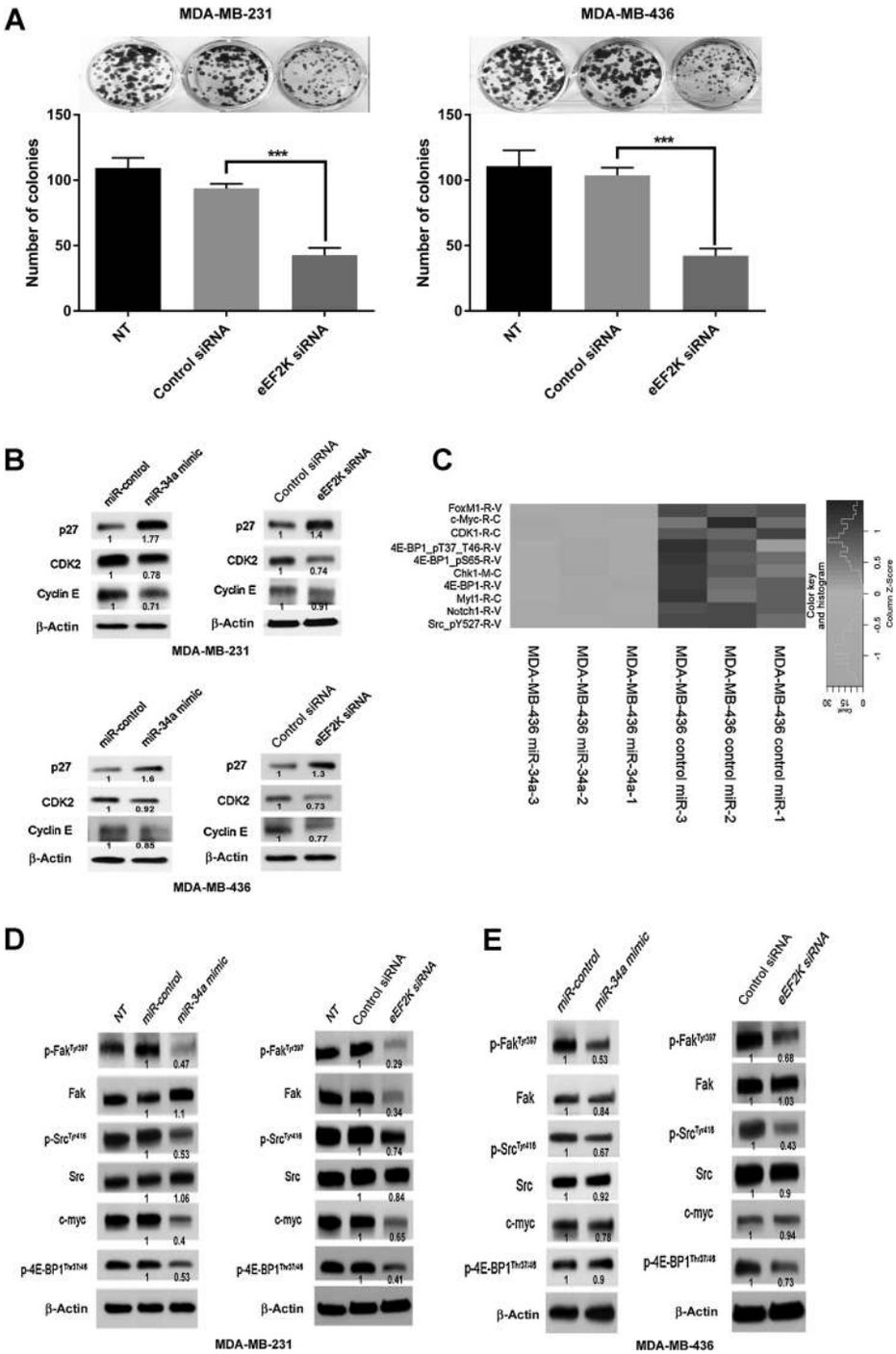

Figure 3.

miR-34a recapitulates the effects of silencing eEF2K on proliferation and migration/invasion markers in TNBC cells. **A,** The effect of eEF2K silencing through transfection with eEF2K siRNA or control siRNA on MDA-MB-231 and MDA-MB-436 cells was determined by a colony-forming assay. Top panels are representative images of the colony culture plates and bottom panels represent quantification of the number of colonies formed. The data are mean ± SDs. ***, $P < 0.001$. **B,** Expression levels of p27, cyclin E1, and CDK2 were determined by the Western blot analysis in MDA-MB-231 and MDA-MB-436 cells in which miR-34a was ectopically expressed or eEF2K silenced by siRNA. β-Actin was used as a loading control. **C,** Heat map of RPPA results showing eEF2K-related proteins altered by miR-34a in MDA-MB-436 cells. The red color indicates the higher expression level of that protein. The green color indicates that the expression level was reduced in miR-34a–transfected cells than in control miRNA–transfected cells. **D** and **E,** Expression levels of p-FAK^{Tyr397}, total FAK, p-SRC^{Tyr416}, total SRC, c-myc, and p-4E-BP1 were determined by the Western blot analysis in MDA-MB-231 and MBDA-MB-436 cells 72 hours after transfection of miR-34a or silencing of eEF2K with siRNA.

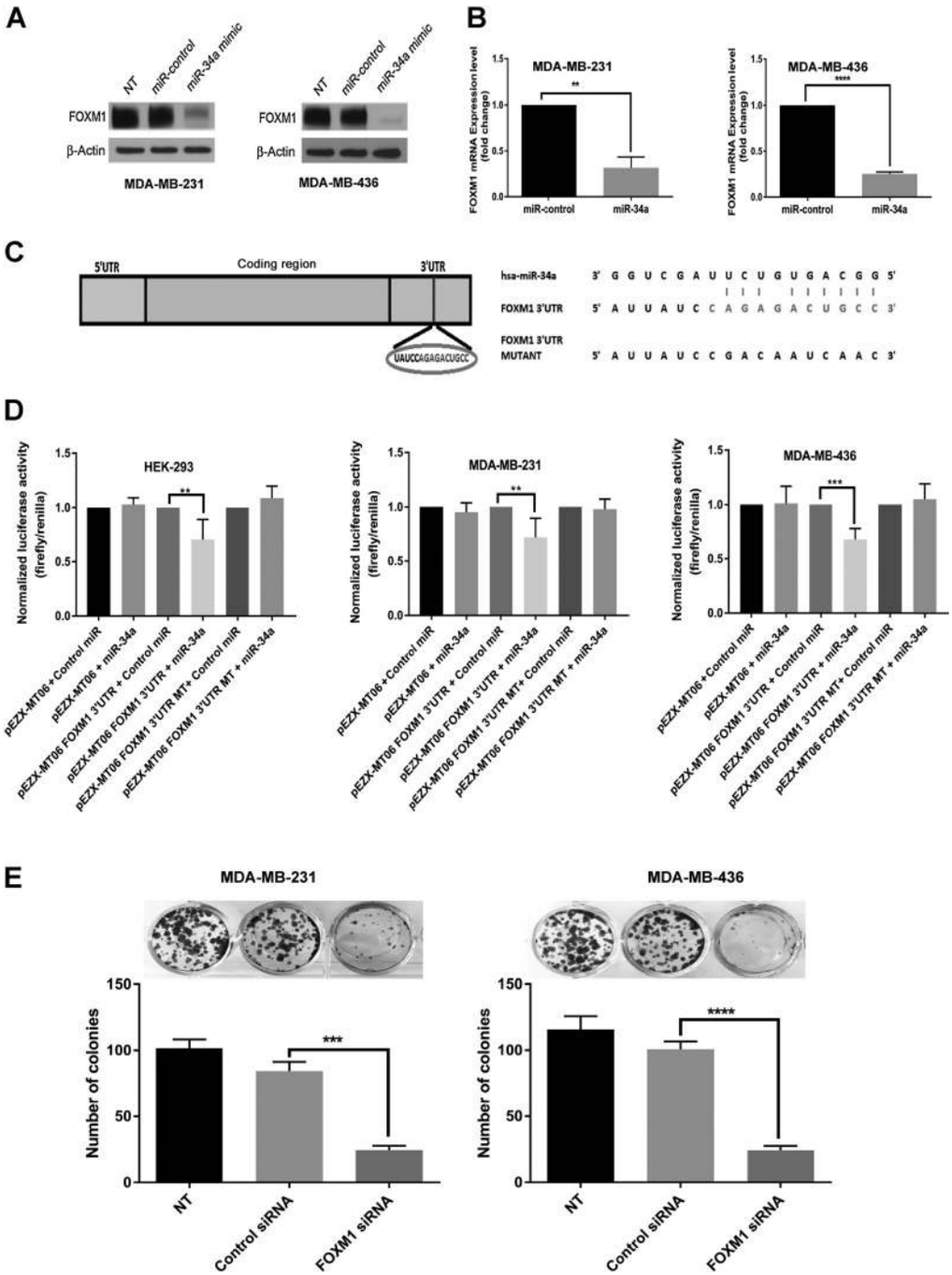

Figure 4.

miR-34a directly binds to 3′-UTR of *FOXM1* mRNA and suppresses its expression and inhibits clonogenic cell growth. **A,** Ectopic overexpression of miR-34a decreased FOXM1 protein expression in MDA-MB-231 and MDA-MB-436 cells as shown by the Western blot analysis. **B,** Ectopic expression of miR-34a in MDA-MB-231 and MDA-MB-436 cells led to decreased *FOXM1* mRNA expression levels by qRT-PCR. **C,** Predicted binding site of miR-34a in the 3′-UTR of human wild-type *FOXM1* and mutant type and their sequences were determined. **D,** Luciferase reporter assay results show that miR-34a directly targets the *FOXM1* 3′-UTR-luciferase reporter in HEK-293, MDA-MB-231, and MDA-MB-436 cells. The firefly luciferase activity of the reporter was normalized to the internal *Renilla* luciferase activity. Data are presented as mean + SDs for three independent experiments. **, $P < 0.001$; ***, $P < 0.0001$. **E,** Silencing FOXM1 by siRNA decreased colony formation by TNBC cells (***, $P < 0.0001$).

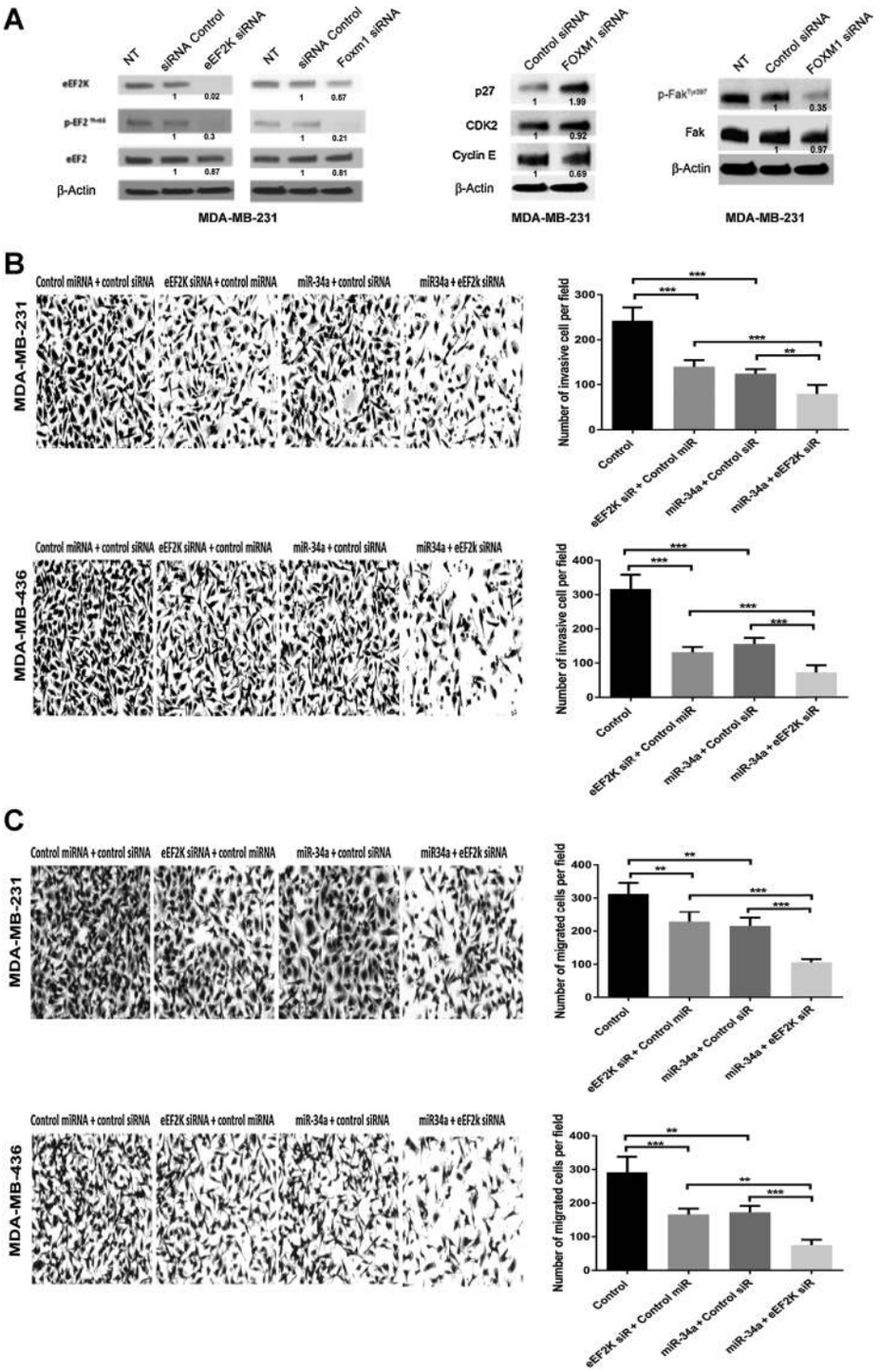

Figure 5.

Effects of FOXM1 and eEF2K silencing on their downstream targets in TNBC cells. **A,** Silencing FOXM1 decreased expression of eEF2K, CDK2, cyclin E, p-FAK^{Tyr397}, and FAK and increased expression of p27 in MDA-MB-231 cells. The Western blot analysis was performed 72 hours after transfection of FOXM1 siRNA**. B,** Inhibition of eEF2K and expression of miR-34a inhibit cell migration and invasion. MDA-MB-231 and MDA-MB-436 cells were transfected with miR-34a, eEF2K siRNA, both, or a combination of miRNA and siRNA controls. Cells were counted in five random fields per well at 40× after 6 hours for migration and after 24 hours for invasion. These representative images show the effect (left). The percentages of migrating or invading cells were calculated compared with those given control treatment (right). **C,** Treatment with miR-34a or eEF2K siRNA significantly decreased the invasive capacities of both cell lines, whereas the combination of both further enhanced the inhibition of cell invasion of the TNBC cells. **, $P < 0.001$; ***, $P < 0.0001$. Treatment with miR-34a or eEF2K siRNA significantly decreased the migration capacities of both cell lines, whereas the combination of both further enhanced the inhibition of cell migration of the TNBC cells. **, $P < 0.001$; ***, $P < 0.0001$.

mediated eEF2K inhibition and tumor suppression. Treatment with the combination of miR-34a and eEF2K siRNA resulted in less invasion and migration by MDA-MB-231 and MDA-MB-436 cells than either miR-34a or *eEF2K* siRNA alone or the controls (Fig. 5B and C). These results suggest that a combination of miR-34a and *eEF2K*-silencing approaches could offer a dual inhibitory effect on TNBC cells and concurrent modulation of other oncogenic members of the same pathway.

eEF2K and FOXM1 overexpression reverse the miR-34a–mediated downstream effects

To further confirm that miR-34a mediates its inhibitory effects through downregulation of eEF2K and FOXM1, we determined whether lentivirus-based overexpression of eEF2K and FOXM1 could reverse the effect of miR-34a–mediated effects. eEF2K overexpression reversed the effects of miR-34a in downregulating FOXM1, p-FAK, and c-myc in MDA-MB-231 cells, whereas only a slight reversal effect in c-myc expression was observed in control-lentivirus and miR-34a–transfected cells (Fig. 6A). In addition, FOXM1 overexpression reversed the effects of miR-34a in downregulating FOXM1 and eEF2K in MDA-MB-231 cells (Supplementary Fig. S2A), suggesting that majority of the effects of miR-34a on eEF2K regulation is mediated by FOXM1 downregulation in TNBC (Fig. 6B). Furthermore, eEF2K and FOXM1 overexpression reversed the effects of miR-34a mimic in MDA-MB-231 cell proliferation and migration and reduced miR-34a–induced inhibition of clonogenic cell growth migration (Fig. 6C; Supplementary Fig. S2B). Moreover, we transfected MDA-MB-231 and MDA-MB-436 cells with miR-34a inhibitor and validated the protein expression level of FOXM1 and eEF2K. Downregulation of miR-34a with inhibitors had no effect on the protein expression of FOXM1 and eEF2K, probably due to very low endogenous levels of miR-34a in these cells. Therefore, inhibition of already very low endogenous miR-34a levels did not induce any further regulatory effects in the cells (Supplementary Fig. S2C).

In vivo therapeutic administration of miR-34a nanoparticles inhibits tumor growth in orthotopic TNBC murine models with human breast cancer xenografts

To determine the *in vivo* effects of miR-34a expression in TNBC tumorigenesis and the therapeutic potential of delivery of this miRNA, we systemically (intravenously) delivered miR-34a in orthotopic MDA-MB-231 and MDA-MB-436 xenograft mouse models. Tumor cells were orthotopically implanted into the mammary fat pad of female nude mice (5 mice/group), and 2 weeks later intravenous injections of dimyristoyl-sn-glycero-3-phosphocholine-based nanoparticles (26, 27) incorporating miR-34a or control miRNA (0.15 mg/kg, i.v., once a week) were started and continued for 4 weeks. The volumes of the xenograft tumors were measured every week for the 4 weeks of treatment. At the end of week 4, tumors were excised and weighed and analyzed for proliferation, angiogenesis, and apoptosis markers by the Western blot analysis. Mice treated with liposomal miR-34a showed significantly less tumor growth than control mice (MDA-MB-231, $P = 0.03$; MDA-MB-436, $P = 0.0296$; Fig. 7A and B). No significant changes in mouse body weights at the end of the treatment period, and no changes in behavioral and eating habits were detected during the 4 weeks of the treatment, suggesting that miR-34a–based gene delivery exerted no or limited side effects (Supplementary Fig. S3A).

The tumor tissues also were analyzed by the Western blot analysis for the effects of miR-34a gene delivery on the expression of FOXM1 and eEF2K levels and its downstream targets. Tumors from miR-34a–treated mice showed reduced expression levels of FOXM1 and eEF2K and its downstream targets p-EF2, c-myc, p-4E-BP1, p-SRC, and p-FAK than tumors from mice treated with control miRNA. miR-34a treatment also decreased expression of *in vivo*, suggesting that miR-34a delivery suppresses FOXM1/EF2K and clinically significant signaling pathways *in vivo* in these models (Supplementary Fig. S3B).

We also assessed the antiproliferative activity of miR-34a on TNBC cells *in vivo* by measuring the expression of the proliferation marker Ki-67 in the excised tumors by IHC analysis. The number of Ki-67–positive tumor cells was significantly lower in tumors of mice treated with miR-34a than in those of mice treated with control miRNA (MDA-MB-231, $P = 0.0011$; MDA-MB-436, $P = 0.0088$; Fig. 7C). Furthermore, miR-34a treatment dramatically decreased microvessel density, as represented by CD31-positive cells, compared with control miRNA (MDA-MB-231, $P = 0.0479$; MDA-MB-436, $P = 0.0388$; Fig. 7D), suggesting its antiangiogenic effect *in vivo* in TNBC mouse models. In addition, miR-34a treatment significantly increased the number of TUNEL-positive cells compared with control miRNA (MDA-MB-231, $P = 0.001$; MDA-MB-436, $P = 0.0084$; Fig. 7E), suggesting that miR-34a has a proapoptotic effect *in vivo*. These results indicate that miR-34a inhibited tumor growth in orthotopic TNBC mouse models through significant suppression of cell proliferation and angiogenesis and induction of apoptosis. Overall, *in vitro* and *in vivo* experiments by RPPA and the Western blot analysis, respectively, in MDA-MB-231 and MDA-MB-436 cells after treatment with miR-34a show alterations in the canonical pathway and multiple interconnected pathways related to cancer signaling (Fig. 8A–C; Supplementary Fig. S4 A–C).

Discussion

The findings presented here suggest that miR-34a is a clinically significant tumor suppressor whose reduced expression is significantly associated with poor clinical outcome and curtailed patient survival in patients with TNBC. Restoration of miR-34a in TNBC cells significantly suppresses FOXM1/eEF2K axis, which is one of the major drivers of TNBC cell proliferation, invasion, and tumor growth and is also highly associated with poor patient survival. Our study also provided the evidence that therapeutic replacement of miR-34a by systemically injected nanodelivery-based gene therapy is safe and inhibits tumor growth in two different TNBC models.

Reports from several laboratories showed that members of the miR-34 family are direct p53 targets, and their upregulation induces apoptosis and cell cycle (30, 31). Recently, Li and colleagues (17) for the first time examined the expression levels of miR-34a in breast cancer tissues from 17 Chinese patients and found that miR-34a was downregulated in 14 compared with corresponding adjacent nonmalignant breast tissues. However, it is unclear in that report which breast cancer subtype was analyzed. Svobada and colleagues (32) investigated expression levels of miR-34a, miR-34b, and miR-34c in samples from 39 patients with TNBC and reported that miR-34b was associated shorter OS, indicating an oncogenic role in TNBC. Zeng and colleagues showed that expressions of miR-34a/b/c were significantly lower in plasma of patients with TNBC compared with healthy

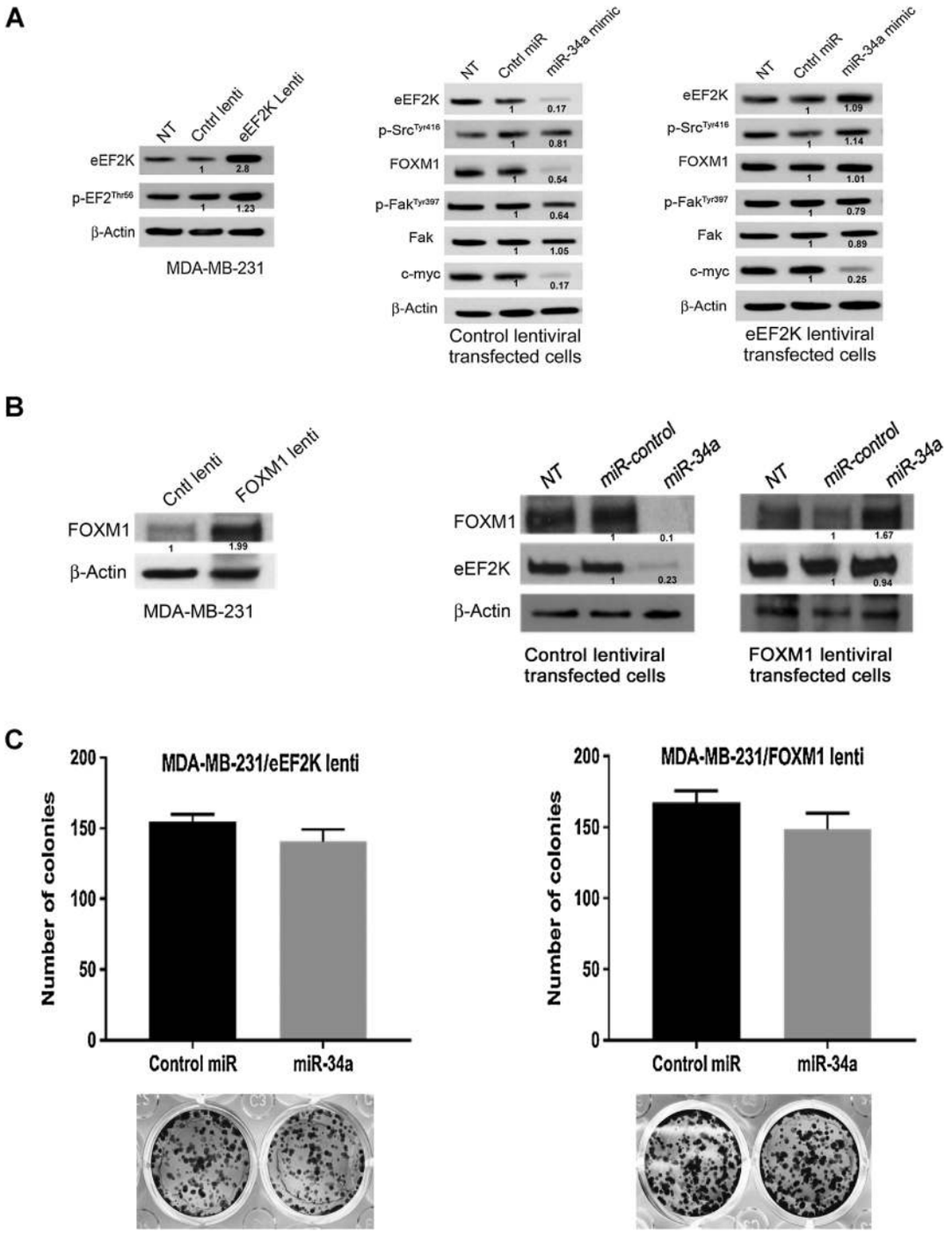

Figure 6.

Overexpression of eEF2K and FOXM1 rescues the effects of miR-34a on TNBC cells. **A** and **B,** MDA-MB-231 cells were transfected with the lentiviral-vector-eEF2K, FOXM1 or control vector, and eEF2K, p-EF2^{Th56}, and FOXM1 protein expression levels were determined by the Western blot analysis to confirm transfection efficiency. NT, no treatment. Treatment with miR-34a mimic in eEF2K-overexpressing MDA-MB-231 cells reversed the effects of eEF2K on proliferation and migration/invasion markers. FOXM1 overexpression reversed the effects of miR-34a in MDA-MB-231 cells and led to reduced inhibition in the expression of FOXM1 and eEF2K. Cells were transfected with miR-34a or control mimic and were analyzed by the Western blot analysis 72 hours later for the expression of eEF2K, FOXM1, p-FAK, and c-myc. β-Actin was used as a loading control. **C,** Overexpression of eEF2K and FOXM1 in MDA-MB-231 cells reversed the effects of miR-34a mimic treatment on clonogenic cell growth.

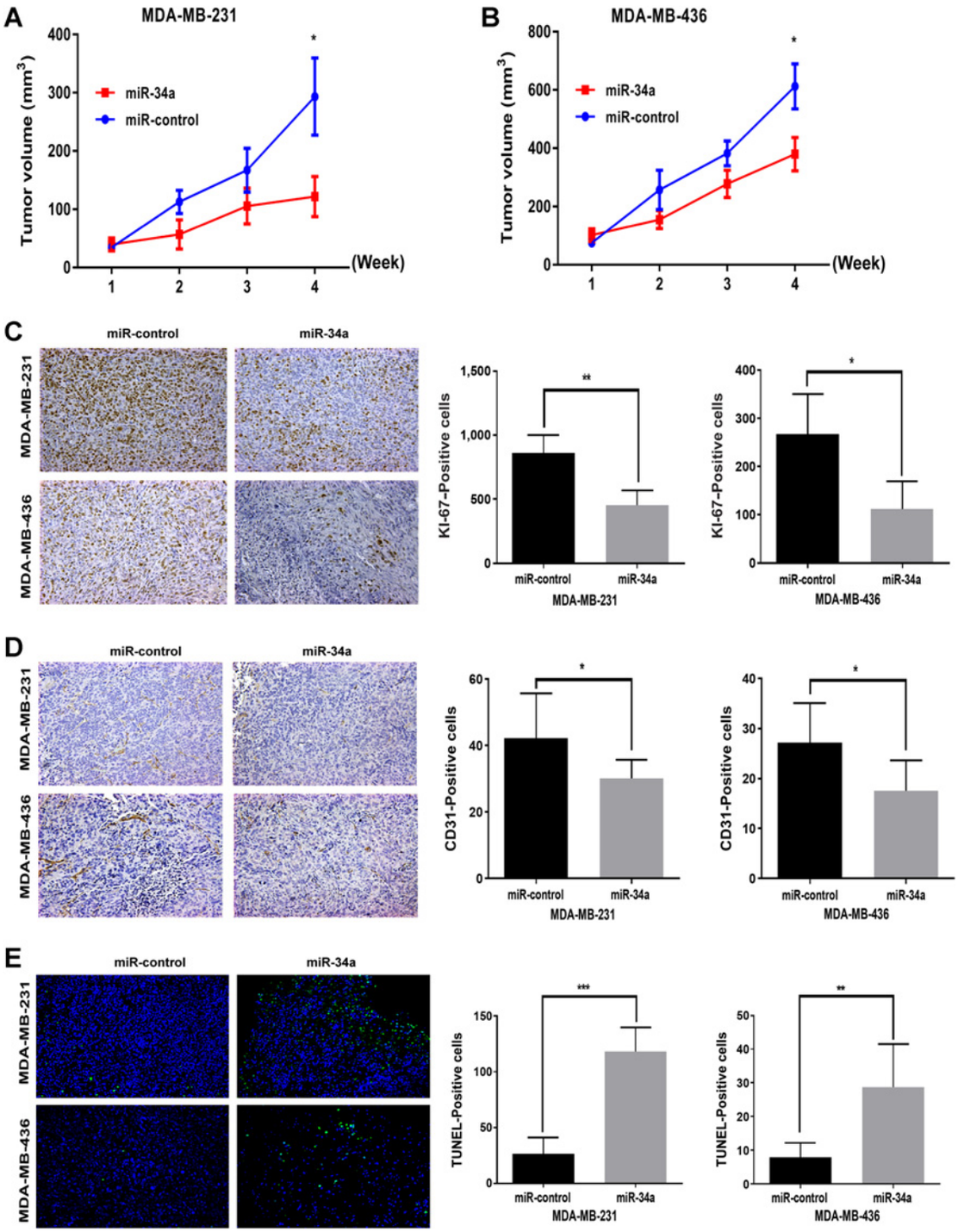

Figure 7.

In vivo systemic administration of nanoparticle-miR-34a inhibits tumor growth and decreases the tumoral expression of FOXM1 and eEF2K and in orthotopic xenograft TNBC models (also see Supplementary Fig. 3B). MDA-MB-231 and MDA-MB-436 tumor-bearing mice were treated with either liposomal nanoparticles incorporating control miRNA (miR-control) or miR-34a mimic [0.3 mg/kg (8 μg/mouse)] intravenously once a week for 4 weeks; 5 mice per group. **A** and **B,** Tumor volumes were measured weekly and are shown as mean ± SDs. **C–E,** Nanoparticle-mediated delivery of miR-34a inhibits tumor cell proliferation and angiogenesis and induces apoptosis in TNBC orthotopic xenograft mouse models. IHC staining was used to evaluate the expression of proliferation marker Ki-67, microvessel density marker CD31, and *in vivo* apoptosis marker TUNEL in MDA-MB-231 and MDA-MB-436 mouse xenografts treated with nanoparticle-miR-34a or control miRNA mimic (miR-control; left). Positively stained cells in both treatment groups were quantified (right; scale bar, 100 μm).

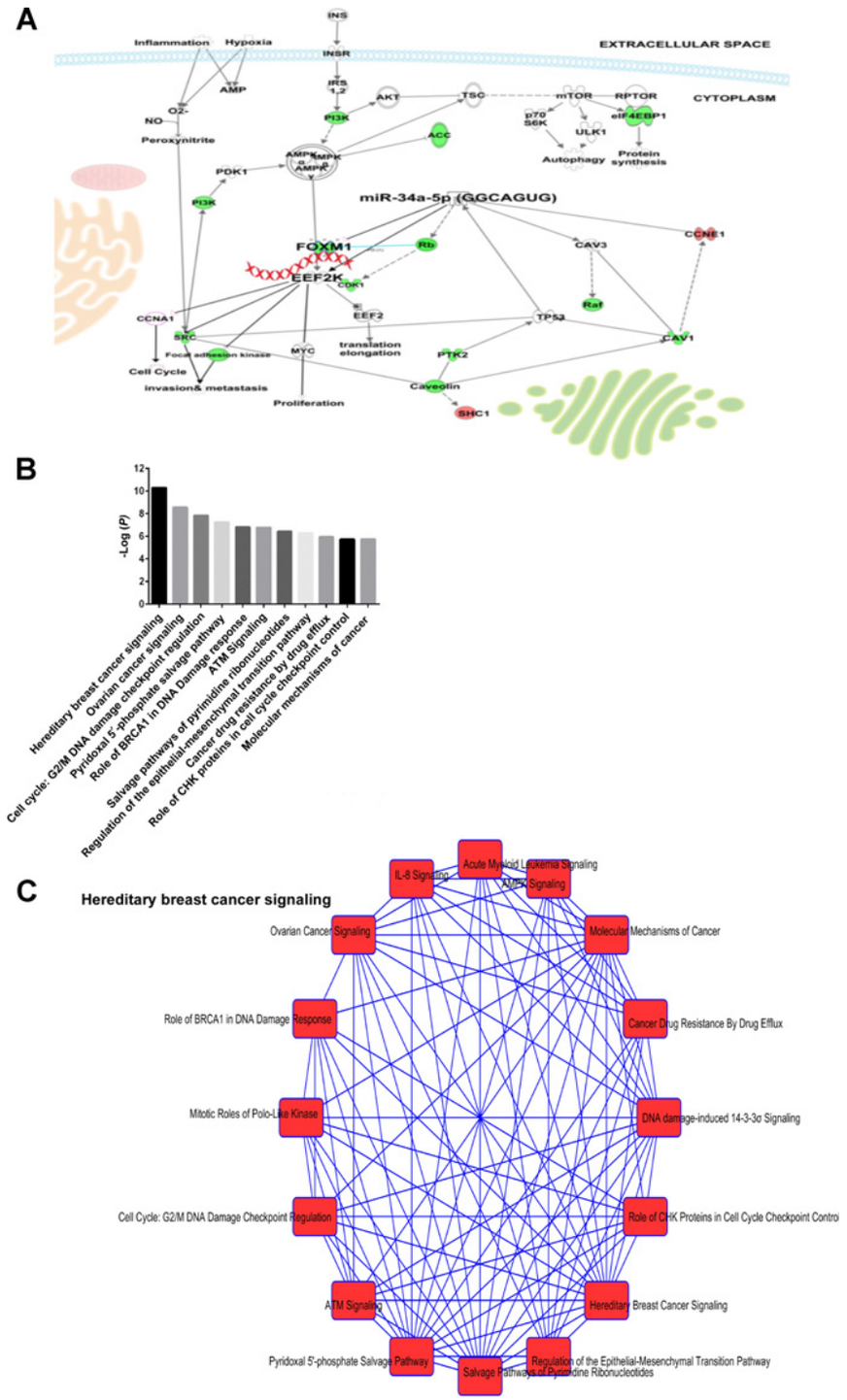

Figure 8.
miR-34a blocks FOXM1/EF2K axis and multiple downstream signaling pathways in TNBC.
A, Ingenuity pathway analysis (IPA) of the canonical pathways/proteins that were significantly altered by ectopic expression of miR-34a in TNBC cells. **B** and **C,** Graphs produced by RPPA analysis of MDA-MB-231 cells treated with miR-34a or control mimic for 72 hours show downregulation of potential target pathways. The canonical pathway analysis showed that multiple interconnected pathways related to cancer signaling were altered upon miR-34a transfection in MDA-MB-231 and MDA-MB-436 cells.

controls (33). In this study, we found that miR-34a expression was significantly lower in TNBC cells compared with normal breast epithelium and that this lower expression was significantly associated with shorter overall patient survival, indicating that miR-34a is a prognostic factor in patients with TNBC. In addition, Imani and colleagues showed that miR-34a inhibits *TWIST1*, *ZEB1*, and *NOTCH1* expression through binding to their 3′-UTR and reduces the metastatic and invasive features of metastatic breast cancer (34, 35). The *TP53* gene (encoding the p53 protein), which is mutated in about 50% of human cancers and 84% of TNBC tumors (36), was shown to induce miR-34, which turned out to be direct p53 target genes (37). Considering the high rate of p53 mutation in TNBC, it is not surprising to detect significantly reduced miR-34a expression in patients with

TNBC. miR-34a has been shown to target and inhibit *Notch1*, *Wnt/β-catenin*, *VEGF*, *HMGA2*, *Rac1*, *c-myc*, *SIRT1*, and *Bcl-2* in various cancers (17–20). However, the molecular mechanisms underlying its tumor suppressor effects are not fully understood. This study indicates that miR-34a exerts the majority of its effects through suppression of FOXM1/eEF2K axis, which we recently showed as one of the major drivers of TNBC tumorigenesis. We previously reported that oncogenic transcription factor FOXM1, which is targeted and suppressed by p53 (38), binds to the promoter of *eEF2K* and regulates its expression, which is associated with poor survival. We have also shown that eEF2K is one of the most important drivers of TNBC tumorigenesis and proposed as a potential molecular target in TNBC (23, 26, 27). eEF2K, an atypical member of the alpha kinase family, is a calcium/calmodulin–-dependent protein kinase that promotes breast cancer cell proliferation, survival, invasion, and drug resistance by inducing clinically relevant oncogenic signaling pathways, including PI3K/AKT, SRC/FAK, IGFR, c-myc, 4E-BP1, cyclin D1, and Bcl-2 in TNBC (39). eEF2K also has been shown to regulate the translocation of peptidyl-tRNA regulate protein synthesis and proposed to contribute to tumor adaptation to nutrient starvation and stress conditions such as hypoxia or acidosis through regulation of protein translation and autophagy (40).

FOXM1 has been proposed as a master regulator of invasion and metastasis, whereas some studies indicate that it is involved in various biological processes, including cell differentiation, survival, cell-cycle progression, DNA damage repair, tissue homeostasis, and angiogenesis (41). Upregulation of FOXM1 expression has been reported to be a result of TP53 mutations in several types of malignancies, including basal/TNBC-type breast cancer, and is associated with advanced tumor stage, high proliferation rate, and poor prognosis (27, 42–46). Therefore, the FOXM1-mediated eEF2K signaling axis functions as one of the major drivers of TNBC and may be targeted for the molecular treatment of these cancers.

Our findings here indicate that the majority of TNBC patient tumors and cell lines have reduced expression of miR-34a, leading to increased eEF2K expression, and thus provides the first evidence of the existence of a p53/miR-34a/FOXM1/eEF2K axis in regulation of tumor growth and progression in TNBC (Supplementary Fig. S5). Increased eEF2K expression contributes to poor patient survival and prognosis by inducing clinically significant pathways and promoting cell proliferation, survival, and drug resistance (PI3K/AKT, c-myc), invasion and metastasis (SRC/FAK), and cell cycle dysregulation. The role of eEF2K in chemoresistance is indicated by the fact that reducing its expression leads to significant enhancement in the efficacy of most widely used chemotherapeutic agents (23). Interestingly, miR-34a induced inhibition of c-myc, a target of eEF2K was not rescued after eEF2K overexpression suggesting that an alternative pathway may regulate its expression.

eEF2K was initially shown to act as a survival factor in response to treatments that induce energy stress and cytotoxic effects through induction of autophagy (47). However, later studies demonstrated that it induces the activity of multiple signaling pathways, including PI3K/Akt, IGFGR, SRC/FAK, integrin β1, c-myc, and cyclin D1, promoting cell proliferation, survival, migration/invasion, and tumorigenesis. This study shows that replacement of miR-34a expression recapitulates the effects of eEF2K suppression in TNBC, including inhibition of tumor cell proliferation, migration, invasion, and tumor growth. Most importantly, the inhibition of tumor growth *in vivo* in an orthotopic xenograft mouse model of TNBC via lipid-based nanoparticle delivery of miR-34a suggests that strategies targeting the miR-34a/eEF2K axis may provide broad antitumor effects through inhibition of multiple oncogenic pathways (Fig. 8A–C).

Recently, miR-34a–based therapeutics (MRX34) were translated into clinical trials by Mirna Therapeutics. However, the study was terminated due to immune-related complications in patients. Studies demonstrated that miR-34a is upregulated following TCR 9 T-cell receptor stimulation. Moreover, miR-34a suppresses the expression of DGKζ, suggesting that miR-34a may function as an inhibitor of DGKζ to enhance T cell activation (48). Although miRNAs can regulate multiple genes simultaneously and lead to toxicicty (49), the lack of specificity of delivery system might be responsible from unexpected side effect as seen in siRNA clinical trials (49–51). In our study, administration of liposomal miR-34a into nude mice with bearing TNBC tumors for 4 weeks did not lead to any side effects. More importantly, injection of liposomal miR-34a into immunocompetent mice at therapeutic concentrations (0.3 mg/kg, i.v.) did not cause any changes in blood chemistry and toxicity markers of kidney, liver, and hematologic cells, including Creatinine, BUN, AST, AST, LDH, and serum glucose levels, suggesting that tumor targeted delivery system is critical to prevention of potential miR-induced side effects (Supplementary Table S3).

Because combining EF2K-targeted therapy with chemotherapeutics such as paclitaxel or doxorubicin may provide significant enhancement of these agents' antitumor efficacy in TNBC models, miR-34a–based therapy could be a potential therapeutic strategy to sensitize tumors to these commonly used chemotherapeutics. Given that reinstatement of miR-34a expression in TNBC is associated with inhibition of tumor growth and downregulation of the axis, strategies involving effective and tumor-specific delivery of miR-34a may be a potential therapeutic approach against TNBC. Because miRNAs have a role in cancer development and their expression is reduced in various cancers, including TNBC, reconstitution of tumor suppressor miRNAs may provide a highly useful therapeutic tool for targeting multiple pathways, including eEF2K.

In conclusion, the results presented here indicate that miR-34a acts as a tumor suppressor that can attenuate the proliferation and invasion of TNBC by directly targeting eEF2K and FOXM1 expression. Restoration of miR-34a or targeting the FOXM1/eEF2K axis may be a potential therapeutic approach against TNBC.

Disclosure of Potential Conflicts of Interest

No potential conflicts of interest were disclosed.

Authors' Contributions

Conception and design: R. Bayraktar, G. Lopez-Berestein, B. Ozpolat

Development of methodology: R. Bayraktar, E. Bayraktar, H.A. Mokhlis, S. Wong, B. Ozpolat

Acquisition of data (provided animals, acquired and managed patients, provided facilities, etc.): R. Bayraktar, G. Lopez-Berestein, G.A. Calin, B. Ozpolat

Analysis and interpretation of data (e.g., statistical analysis, biostatistics, computational analysis): R. Bayraktar, C. Ivan, P. Kanlikilicer, N. Kahraman, J. Sheng, S. Wong

Writing, review, and/or revision of the manuscript: R. Bayraktar, E. Bayraktar, N.N. Kabil, C. Rodriguez-Aguayo, A. Arslan, G. Lopez-Berestein, G.A. Calin, B. Ozpolat

Administrative, technical, or material support (i.e., reporting or organizing data, constructing databases): R. Bayraktar, E. Bayraktar, D. Karakas, B. Ozpolat
Study supervision: B. Ozpolat

Acknowledgments

This work was supported in part by grants from the NIH/NCI (R21CA199050 and P30CA016672) and the funding from noncoding RNA center and used the Functional Proteomics RPPA Core Facility.

The costs of publication of this article were defrayed in part by the payment of page charges. This article must therefore be hereby marked *advertisement* in accordance with 18 U.S.C. Section 1734 solely to indicate this fact.

Received July 11, 2017; revised November 30, 2017; accepted May 2, 2018; published first May 10, 2018.

References

1. Bauer KR, Brown M, Cress RD, Parise CA, Caggiano V. Descriptive analysis of estrogen receptor (ER)-negative, progesterone receptor (PR)-negative, and HER2-negative invasive breast cancer, the so-called triple-negative phenotype: a population-based study from the California cancer Registry. Cancer 2007;109:1721–8.
2. Dent R, Trudeau M, Pritchard KI, Hanna WM, Kahn HK, Sawka CA, et al. Triple-negative breast cancer: clinical features and patterns of recurrence. Clin Cancer Res 2007;13:4429–34.
3. Kohler BA, Sherman RL, Howlader N, Jemal A, Ryerson AB, Henry KA, et al. Annual report to the nation on the status of cancer,1975–2011, featuring incidence of breast cancer subtypes by race/ethnicity, poverty, and state. J Natl Cancer Inst 2015;107:djv048.
4. Foulkes WD, Smith IE, Reis-Filho JS. Triple-negative breast cancer. N Engl J Med 2010;363:1938–48.
5. Haffty BG, Yang Q, Reiss M, Kearney T, Higgins SA, Weidhaas J, et al. Locoregional relapse and distant metastasis in conservatively managed triple negative early-stage breast cancer. J Clin Oncol 2006; 24:5652–7.
6. Malorni L, Shetty PB, De Angelis C, Hilsenbeck S, Rimawi MF, Elledge R, et al. Clinical and biologic features of triple-negative breast cancers in a large cohort of patients with long-term follow-up. Breast Cancer Res Treat 2012;136:795–804.
7. Bartel DP. MicroRNAs: target recognition and regulatory functions. Cell 2009;136:215–33.
8. Bayraktar R, Van Roosbroeck K. miR-155 in cancer drug resistance and as target for miRNA-based therapeutics. Cancer Metastasis Rev 2018; 37:33–44.
9. Chang TC, Wentzel EA, Kent OA, Ramachandran K, Mullendore M, Lee KH, et al. Transactivation of miR-34a by p53 broadly influences gene expression and promotes apoptosis. Mol Cell 2007;26: 745–52.
10. Hermeking H. The miR-34 family in cancer and apoptosis. Cell Death Differ 2010;17:193–9.
11. Liu C, Kelnar K, Liu B, Chen X, Calhoun-Davis T, Li H, et al. The microRNA miR-34a inhibits prostate cancer stem cells and metastasis by directly repressing CD44. Nat Med 2011;17:211–5.
12. Mangala LS, Wang H, Jiang D, Wu SY, Somasunderam A, Volk DE, et al. Improving vascular maturation using noncoding RNAs increases antitumor effect of chemotherapy. JCI insight 2016;1:e87754.
13. Rashed MH, Kanlikilicer P, Rodriguez-Aguayo C, Pichler M, Bayraktar R, Bayraktar E, et al. Exosomal miR-940 maintains SRC-mediated oncogenic activity in cancer cells: a possible role for exosomal disposal of tumor suppressor miRNAs. Oncotarget 2017;8:20145–64.
14. Rodriguez-Aguayo C, Monroig PDC, Redis RS, Bayraktar E, Almeida MI, Ivan C, et al. Regulation of hnRNPA1 by microRNAs controls the miR-18a-K-RAS axis in chemotherapy-resistant ovarian cancer. Cell Discov 2017; 3:17029.
15. Corney DC, Hwang CI, Matoso A, Vogt M, Flesken-Nikitin A, Godwin AK, et al. Frequent downregulation of miR-34 family in human ovarian cancers. Clin Cancer Res 2010;16:1119–28.
16. Ji Q, Hao X, Zhang M, Tang W, Yang M, Li L, et al. MicroRNA miR-34 inhibits human pancreatic cancer tumor-initiating cells. PLoS One 2009;4: e6816.
17. Li L, Yuan L, Luo J, Gao J, Guo J, Xie X. MiR-34a inhibits proliferation and migration of breast cancer through down-regulation of Bcl-2 and SIRT1. Clin Exp Med 2013;13:109–17.
18. Li Y, Guessous F, Zhang Y, Dipierro C, Kefas B, Johnson E, et al. MicroRNA-34a inhibits glioblastoma growth by targeting multiple oncogenes. Cancer Res 2009;69:7569–76.
19. Si W, Li Y, Shao H, Hu R, Wang W, Zhang K, et al. MiR-34a inhibits breast cancer proliferation and progression by targeting Wnt1 in Wnt/beta-catenin signaling pathway. Am J Med Sci 2016;352:191–9.
20. Yamakuchi M, Ferlito M, Lowenstein CJ. miR-34a repression of SIRT1 regulates apoptosis. Proc Natl Acad Sci U S A 2008;105:13421–6.
21. ClinicalTrials.gov. NCT02862145. Available from: https://clinicaltrials.gov/.
22. Ryazanov AG, Ward MD, Mendola CE, Pavur KS, Dorovkov MV, Wiedmann M, et al. Identification of a new class of protein kinases represented by eukaryotic elongation factor-2 kinase. Proc Natl Acad Sci U S A 1997; 94:4884–9.
23. Tekedereli I, Alpay SN, Tavares CD, Cobanoglu ZE, Kaoud TS, Sahin I, et al. Targeted silencing of elongation factor 2 kinase suppresses growth and sensitizes tumors to doxorubicin in an orthotopic model of breast cancer. PLoS One 2012;7:e41171.
24. Shahbazi R, Asik E, Kahraman N, Turk M, Ozpolat B, Ulubayram K. Modified gold-based siRNA nanotherapeutics for targeted therapy of triple-negative breast cancer. Nanomedicine 2017; 12:1961–73.
25. D'Andrade PN, Fulmer-Smentek S. Agilent microRNA microarray profiling system. Methods Mol Biol 2012;822:85–102.
26. Bayraktar R, Pichler M, Kanlikilicer P, Ivan C, Bayraktar E, Kahraman N, et al. MicroRNA 603 acts as a tumor suppressor and inhibits triple-negative breast cancer tumorigenesis by targeting elongation factor 2 kinase. Oncotarget 2017;8:11641–58.
27. Hamurcu Z, Ashour A, Kahraman N, Ozpolat B. FOXM1 regulates expression of eukaryotic elongation factor 2 kinase and promotes proliferation, invasion and tumorgenesis of human triple negative breast cancer cells. Oncotarget 2016;7:16619–35.
28. Kanlikilicer P, Rashed MH, Bayraktar R, Mitra R, Ivan C, Aslan B, et al. Ubiquitous release of exosomal tumor suppressor miR-6126 from ovarian cancer cells. Cancer Res 2016;76:7194–207.
29. Xu X, Chen W, Miao R, Zhou Y, Wang Z, Zhang L, et al. miR-34a induces cellular senescence via modulation of telomerase activity in human hepatocellular carcinoma by targeting FoxM1/c-Myc pathway. Oncotarget 2015;6:3988–4004.
30. He L, He X, Lim LP, de Stanchina E, Xuan Z, Liang Y, et al. A microRNA component of the p53 tumour suppressor network. Nature 2007;447: 1130–4.
31. Raver-Shapira N, Marciano E, Meiri E, Spector Y, Rosenfeld N, Moskovits N, et al. Transcriptional activation of miR-34a contributes to p53-mediated apoptosis. Mol Cell 2007;26:731–43.
32. Svoboda M, Sana J, Redova M, Navratil J, Palacova M, Fabian P, et al. MiR-34b is associated with clinical outcome in triple-negative breast cancer patients. Diagn Pathol 2012;7:31.
33. Zeng Z, Chen X, Zhu D, Luo Z, Yang M. Low expression of circulating microRNA-34c is associated with poor prognosis in triple-negative breast cancer. Yonsei Med J 2017;58:697–702.
34. Imani S, Wei C, Cheng J, Khan MA, Fu S, Yang L, et al. MicroRNA-34a targets epithelial to mesenchymal transition-inducing transcription factors (EMT-TFs) and inhibits breast cancer cell migration and invasion. Oncotarget 2017;8:21362–79.
35. Imani S, Zhang X, Hosseinifard H, Fu S, Fu J. The diagnostic role of microRNA-34a in breast cancer: a systematic review and meta-analysis. Oncotarget 2017;8:23177–87.
36. Cancer Genome Atlas Research Network, Kandoth C, Schultz N, Cherniack AD, Akbani R, Liu Y, et al. Integrated genomic characterization of endometrial carcinoma. Nature 2013;497:67–73.
37. Navarro F, Lieberman J. miR-34 and p53: new insights into a complex functional relationship. PLoS One 2015;10:e0132767.

38. Barsotti AM, Prives C. Pro-proliferative FoxM1 is a target of p53-mediated repression. Oncogene 2009;28:4295–305.
39. Kenney JW, Moore CE, Wang X, Proud CG. Eukaryotic elongation factor 2 kinase, an unusual enzyme with multiple roles. Adv Biol Regul 2014;55: 15–27.
40. Leprivier G, Remke M, Rotblat B, Dubuc A, Mateo AR, Kool M, et al. The eEF2 kinase confers resistance to nutrient deprivation by blocking translation elongation. Cell 2013;153:1064–79.
41. Koo CY, Muir KW, Lam EW. FOXM1: from cancer initiation to progression and treatment. Biochim Biophys Acta 2012;1819:28–37.
42. Curtis C, Shah SP, Chin SF, Turashvili G, Rueda OM, Dunning MJ, et al. The genomic and transcriptomic architecture of 2,000 breast tumours reveals novel subgroups. Nature 2012;486:346–52.
43. Halasi M, Gartel AL. FOX(M1) news—it is cancer. Mol Cancer Ther 2013; 12:245–54.
44. Halasi M, Gartel AL. Targeting FOXM1 in cancer. Biochem Pharmacol 2013;85:644–52.
45. Katoh M, Igarashi M, Fukuda H, Nakagama H, Katoh M. Cancer genetics and genomics of human FOX family genes. Cancer Lett 2013;328:198–206.
46. Liu M, Dai B, Kang SH, Ban K, Huang FJ, Lang FF, et al. FoxM1B is overexpressed in human glioblastomas and critically regulates the tumorigenicity of glioma cells. Cancer Res 2006;66:3593–602.
47. Zhu H, Yang X, Liu J, Zhou L, Zhang C, Xu L, et al. Eukaryotic elongation factor 2 kinase confers tolerance to stress conditions in cancer cells. Cell Stress Chaperones 2015;20:217–20.
48. Shin J, Xie D, Zhong XP. MicroRNA-34a enhances T cell activation by targeting diacylglycerol kinase zeta. PLoS One 2013;8:e77983.
49. Bayraktar R, Van Roosbroeck K, Calin GA. Cell-to-cell communication: microRNAs as hormones. Mol Oncol 2017;11:1673–86.
50. Ozcan G, Ozpolat B, Coleman RL, Sood AK, Lopez-Berestein G. Preclinical and clinical development of siRNA-based therapeutics. Adv Drug Deliv Rev 2015;87:108–19.
51. Ozpolat B, Sood AK, Lopez-Berestein G. Liposomal siRNA nanocarriers for cancer therapy. Adv Drug Deliv Rev 2014;66:110–6.